

The role of cathepsin D in the pathophysiology of heart failure and its potentially beneficial properties: a translational approach

Martijn F. Hoes^{1†}, Jasper Tromp^{1,2,3†}, Wouter Ouwerkerk^{2,4}, Nils Bomer¹, Silke U. Oberdorf-Maass¹, Nilesh J. Samani⁵, Leong L. Ng⁵, Chim C. Lang⁶, Pim van der Harst¹, Hans Hillege¹, Stefan D. Anker^{7,8,9}, Marco Metra¹⁰, Dirk J. van Veldhuisen¹, Adriaan A. Voors¹, and Peter van der Meer^{1*}

¹Department of Cardiology, University of Groningen, Groningen, The Netherlands; ²National Heart Centre Singapore, Singapore; ³Duke-NUS Medical School, Singapore; ⁴Department of Epidemiology, Biostatistics & Bioinformatics, Academic Medical Center, Amsterdam, The Netherlands; ⁵Department of Cardiovascular Sciences, University of Leicester, and NIHR Leicester Biomedical Research Centre, Glenfield Hospital, Leicester, UK; ⁶Division of Molecular & Clinical Medicine, University of Dundee, Dundee, UK; ⁷Division of Cardiology and Metabolism – Heart Failure, Cachexia & Sarcopenia; Department of Cardiology (CVK); and Berlin-Brandenburg Center for Regenerative Therapies (BCRT), Charité University Medicine, Berlin, Germany; ⁸Department of Cardiology and Pneumology, University Medicine Göttingen (UMG), Göttingen, Germany; ⁹DZHK (German Center for Cardiovascular Research), Berlin, Germany; and ¹⁰Institute of Cardiology, Department of Medical and Surgical Specialties, Radiological Sciences and Public Health, University of Brescia, Brescia, Italy

Received 12 February 2019; revised 17 October 2019; accepted 18 October 2019; online publish-ahead-of-print 3 December 2019

Aims

Cathepsin D is a ubiquitous lysosomal protease that is primarily secreted due to oxidative stress. The role of circulating cathepsin D in heart failure (HF) is unknown. The aim of this study is to determine the association between circulating cathepsin D levels and clinical outcomes in patients with HF and to investigate the biological settings that induce the release of cathepsin D in HF.

Methods and results

Cathepsin D levels were studied in 2174 patients with HF from the BIOSTAT-CHF index study. Results were validated in 1700 HF patients from the BIOSTAT-CHF validation cohort. The primary combined outcome was all-cause mortality and/or HF hospitalizations. Human pluripotent stem cell-derived cardiomyocytes were subjected to hypoxic, pro-inflammatory signalling and stretch conditions. Additionally, cathepsin D expression was inhibited by targeted short hairpin RNAs (shRNA). Higher levels of cathepsin D were independently associated with diabetes mellitus, renal failure and higher levels of interleukin-6 and N-terminal pro-B-type natriuretic peptide ($P < 0.001$ for all). Cathepsin D levels were independently associated with the primary combined outcome [hazard ratio (HR) per standard deviation (SD): 1.12; 95% confidence interval (CI) 1.02–1.23], which was validated in an independent cohort (HR per SD: 1.23, 95% CI 1.09–1.40). *In vitro* experiments demonstrated that human stem cell-derived cardiomyocytes released cathepsin D and troponin T in response to mechanical stretch. ShRNA-mediated silencing of cathepsin D resulted in increased necrosis, abrogated autophagy, increased stress-induced metabolism, and increased release of troponin T from human stem cell-derived cardiomyocytes under stress.

Conclusions

Circulating cathepsin D levels are associated with HF severity and poorer outcome, and reduced levels of cathepsin D may have detrimental effects with therapeutic potential in HF.

Keywords

Heart failure • Cathepsin D • Biomarkers • Human stem cell-derived cardiomyocytes • BIOSTAT-CHF

*Corresponding author. Department of Cardiology, University Medical Center Groningen, Hanzeplein 1, PO Box 30.001, 9700 RB Groningen, The Netherlands. Tel: +31 50 3612355, Fax: +31 50 3611347, Email: p.van.der.meer@umcg.nl

†These authors contributed equally.

Introduction

Oxidative stress is an important pathophysiological pathway in the development and progression of heart failure (HF).^{1–3} Oxidative stress occurs when the balance between production of reactive oxygen species and endogenous antioxidative mechanisms fails.^{1,4,5}

The aspartyl protease cathepsin D is a ubiquitously expressed lysosomal enzyme that is essential for protein degradation, proteolytic activation of hormones and growth factors, and is primarily secreted following oxidative stress.^{6–8} Cathepsin D is a member of the A1 family of peptidases and is composed of a light and a heavy chain that together form the fully active mature enzyme.^{9,10} Recent data showed that cathepsin D was upregulated in a myocardial infarction model. Furthermore, upregulating cathepsin D was cardioprotective and prevented the development of HF.^{11,12} In addition, high circulating levels of cathepsin D are associated with increased risk of coronary events and new-onset HF following ST-segment elevation acute myocardial infarction.^{13,14} The cause for cathepsin D release and whether levels of cathepsin D are associated with clinical outcomes in the general HF population is currently unknown.

Therefore, in the present study, we investigated the association between circulating cathepsin D levels and clinical variables as well as cardiovascular outcome. To assess what type of stress induces cathepsin D release from cardiomyocytes, we measured extracellular cathepsin D levels from human stem cell-derived cardiomyocyte (as a proxy for human cardiomyocytes *in vivo*) in human cardiac *in vitro* models of ventricular wall stress, hypoxia (i.e. ischaemia) and inflammation. Finally, we assessed how inhibition of intracellular cathepsin D expression affects human stem cell-derived cardiomyocyte survival after stress.

Methods

Patient population and study design

The current study was performed as a sub-study of the BIOlogy Study to Tailored Treatment in Chronic Heart Failure (BIOSTAT-CHF).^{15–18} In short, the BIOSTAT-CHF study includes two cohorts of patients with HF. The index cohort consists of 2516 patients with HF from 69 centres in 11 European countries. Inclusion criteria for the index cohort include: patients with ≥ 18 years of age, having symptoms of new-onset or worsening HF as confirmed by a left ventricular ejection fraction (LVEF) of $\leq 40\%$. Additionally, patients with LVEF $> 40\%$ were enrolled in the BIOSTAT-CHF study, but were required to have a B-type natriuretic peptide > 400 pg/mL or an N-terminal pro-B-type natriuretic peptide (NT-proBNP) > 2000 pg/mL. Patients in the index and validation cohort were required to be sub-optimally treated on either angiotensin-converting enzyme inhibitors/angiotensin receptor blockers (ACEi/ARBs) and/or beta-blockers, or they received $\leq 50\%$ of ACEi/ARB and/or beta-blockers at the time of inclusion and anticipated initiation/up-titration of ACEi/ARBs and beta-blockers.

The validation cohort consists of 1738 patients from six centres in Scotland, UK. Patients were included if they were ≥ 18 years of age, diagnosed with HF and were previously admitted with HF requiring diuretic treatment. They were sub-optimally treated with

ACEi/ARBs and/or beta-blockers, and anticipated initiation or up-titration of ACEi/ARBs and beta-blockers.

Study definitions and measurements

Medical history, medication use and physical examination were recorded at baseline. Overall, 91% of patients in the index cohort had echocardiography performed < 6 months before inclusion. Changes in ACEi/ARB and beta-blocker usage were recorded. HF with a reduced ejection fraction (HFrEF) was defined as an LVEF $\leq 40\%$, HF with a mid-range ejection fraction (HFmrEF) was defined as an LVEF of 41–49%, and HF with a preserved ejection fraction (HFpEF) was defined as an LVEF $\geq 50\%$. Co-morbidities were identified by chart review from medical history, anaemia was defined according to World Health Organization definitions with a sex specific cutoff point for haemoglobin (< 13 g/dL in males and < 12 g/dL in females).

Outcome

The primary outcome of this study was a combined outcome of all-cause mortality and HF hospitalizations at 2 years. The secondary outcome was all-cause mortality at 2 years. The cause of hospitalization was determined by the individual site investigators.

Biomarkers

Circulating plasma levels were determined using the Olink Proseek[®] Multiplex Cardiovascular III^{96x96} kit by the Olink Bioscience analysis service (Uppsala, Sweden) as described previously.^{16,19,20} The kit is based on the Proximity Extension Assay (PEA) technology that binds oligonucleotide-labelled antibody probe pairs to the respective target in the sample. Proseek[®] data are presented as arbitrary units (AU) for normalized protein expression. The inter- and intra-assay coefficients of variation are 6.6% and 10.3%, respectively. The lower limit of detection was 976.6 pg/mL. Due to the nature of the measurement using PEA technology, cathepsin D was expressed as relative AU, where higher values correspond to higher levels of cathepsin D.

Cell culture and differentiation

HUES9 human pluripotent stem cells (hPSC; Harvard Stem Cell Institute) were maintained and differentiated as published previously.²¹ Briefly, hPSC were maintained in Essential 8 medium (A1517001; Thermo Fisher Scientific) before differentiation to stem cell-derived cardiomyocytes (hPSC-CM) was initiated, which was achieved by culturing hPSC in RPMI1640 medium (21875–034, Thermo Fisher Scientific) supplemented with 1x B27 minus insulin (Thermo Fisher Scientific) and 6 $\mu\text{mol/L}$ CHIR99021 (13 122, Cayman Chemical). After 2 days, medium was refreshed with RPMI1640 supplemented with 1x B27 minus insulin and 2 $\mu\text{mol/L}$ Wnt-C59 (5148, Tocris Bioscience). Again after 2 days, medium was changed to CDM3 medium as described by BurrIDGE *et al.*²² and was refreshed every other day. On day 8 after induction of differentiation, spontaneously contracting cardiomyocytes were observed, which were subsequently purified by changing the medium to glucose-free CDM3 medium supplemented with 5 mmol/L sodium DL-lactate (CDM3L; Sigma-Aldrich), as published by BurrIDGE *et al.*²² Ultimately, this resulted in $> 99\%$ pure spontaneously beating stem cell-derived cardiomyocyte cultures.

Cardiomyocyte stimulation

Obtained human cardiomyocytes were seeded on a flexible surface (BF-3001C, FlexCell) subjected to 15% equiaxial mechanical stretch at 1 Hz for 24 h or 48 h using a FX-4000 system (FlexCell) as mentioned previously.²³ Cardiomyocytes were cultured in anaerobic pouches (260 683, BD) for 72 h to create hypoxic conditions. Additionally, cardiomyocytes were incubated with 100 ng/mL tumour necrosis factor alpha (TNF α ; SRP3177, Sigma-Aldrich) for 72 h in order to mimic an inflammatory environment. To inhibit lysosomal exocytosis, hPSC-CM were incubated with the small molecule vacuolin-1 (20 425, Cayman Chemical) at a concentration of 1 μ M in the cell medium.²⁴

Lentivirus production

HEK-293 T cells were cultured at 37°C and 5% CO₂ until 70% confluency was reached in Dulbecco modified Eagle medium (DMEM; 41 965–039, Thermo Fisher Scientific) supplemented with 10% fetal calf serum (FCS; F7524, Sigma-Aldrich). HEK-293 T were transfected with Fugene HD (E2311, Promega) and a mix of pCMV Δ 8.91-transfer plasmid, VSV-G-packaging plasmid and pLKO.1-plasmid expressing short hairpin RNA (shRNA) against cathepsin D or a non-mammalian scrambled sequence at a ratio of 5:2:6. Media were replaced with fresh CDM3 medium after 24 h. CDM3 medium containing viral particles was harvested and filtered with 0.45 μ m Nalgene filter after 48 h. Clean viral supernatant was used directly or was snap frozen for extended storage. pLKO.1-shCTSD (TRCN000003660, Sigma-Aldrich) and pLKO.1-shSCR (SHC002, Sigma-Aldrich) were purchased from Sigma MISSION RNAi.

Immunoblotting

Protein was isolated in radioimmunoprecipitation assay (RIPA) buffer supplemented with 1% phosphatase inhibitor cocktail 3 (p0044, Sigma-Aldrich), 1x cOmplete protease inhibitor cocktail (11 873 580 001, Roche), and 15 mM sodium orthovanadate (S6508, Sigma-Aldrich). Protein concentration was determined with the DC protein assay kit. Equal amounts of protein were separated by SDS-PAGE and proteins were transferred to PVDF membrane. For detection of specific proteins, the following antibodies were used: polyclonal anti-cathepsin D IgG (1:1000; sc-10 725, Santa Cruz), monoclonal anti-Caspase 3 (1:1000; 9664, Cell Signalling) and monoclonal anti-GAPDH IgG (1:30 000; 10R-G109A, Fitzgerald). After washing, blots were incubated with polyclonal goat anti-rabbit IgG-HRP (1:2000; P0448, Dako), and polyclonal rabbit anti-mouse IgG-HRP (1:2000; P0260, Dako). Signals were detected visualized with enhanced chemiluminescence (ECL; NEL120001EA, PerkinElmer) and densitometry has been analysed with ImageQuant LAS 4000 (GE Healthcare). Cathepsin D signals were normalized to respective GAPDH levels.

Cathepsin D and troponin T determination in medium

Medium samples were collected and centrifuged at 12.000 \times g to remove cellular debris. Cathepsin D was determined in the supernatant by enzyme-linked immunosorbent assay (ELISA) according to manufacturer protocols (ab119586, Abcam). Troponin T levels were analysed using an electrochemiluminescence immunoassay kit (0509277, Roche Diagnostics).

Immunocytochemistry and sarcomere classification

Die-cut pieces of stretch plate membrane were washed twice with cold PBS, and fixed with 4% paraformaldehyde on ice during 10 min. Fixed cells were washed three times with PBS, followed by permeabilization with PBS + 0.3% Triton-X100 (T9284, Sigma-Aldrich) on ice during 5 min. Samples were blocked for 1 h at room temperature with PBS/Tween (0.1%; P1379, Sigma-Aldrich) containing 3% BSA (11 930, Serva) and 2% goat serum (G9023, Sigma). Cells were subsequently incubated with monoclonal anti- α -actinin IgG1 (1:100; A7811, Sigma-Aldrich) dissolved in the blocking mix during 1 h. After washing, cells were incubated with Alexa Fluor 555 goat-anti-mouse IgG (1:1000; A21424, Thermo Fisher Scientific). Pieces of membrane were mounted with Vectashield mounting medium containing DAPI (H-1200, Vector labs) and images were obtained with a Leica AF-6000 microscope.

Sarcomere classification was determined as described previously.²⁵ Briefly, images of hPSC-CM acquired after immunocytochemistry were analysed based on three classes of sarcomeric structure: class I sarcomeres showed distinct sarcomeric bands (e.g. as stained positively for α -actinin) that cover >50% of the cell area. Class II sarcomeric structure showed clear sarcomeric bands, but covered <50% of the cell area, while class III sarcomeres showed positive staining for α -actinin, but lacked any band-like structures. Human PSC-CM were classified based on sarcomere structure for each condition.

Apoptosis, necrosis, autophagy and metabolism

Stem cell-derived cardiomyocyte survival (i.e. apoptosis and necrosis), levels of autophagy, and metabolic rates were determined with the RealTime-Glo™ Annexin V Apoptosis and Necrosis Assay kit (JA1011, Promega), the CYTO-ID® Autophagy detection kit 2.0 (ENZ-KIT175-0050, Enzo Life Sciences), and the RealTime-Glo™ MT Cell Viability Assay kit (G9711, Promega) respectively. All assays have been performed according to respective manufacturer protocols on living cells on pieces of flexible membrane that were die-cut from the stretch plates.

Statistical analysis

Levels of cathepsin D in the BIOSTAT-CHF study were divided into tertiles. Following, clinical characteristics between tertiles of cathepsin D were compared using the one-way analysis of variance (ANOVA), Kruskal–Wallis test or the Chi-square test where appropriate. Distribution of continuous data was visually inspected using Q–Q plots. Logistic regression was used to investigate independent associations with the highest tertile of cathepsin D. Differences in outcome were graphically shown using Kaplan–Meier curves. The log-rank test was used to test for difference in survival between tertiles of cathepsin D. Cox regression analyses were used to investigate the linear association between cathepsin D and outcome. We corrected in a step-wise manner for age, sex, body mass index, history of diabetes, and usage of beta-blockers, ACEi and mineralocorticoid receptor antagonists at baseline. Additionally, we corrected for the BIOSTAT-CHF risk engine, which has been published before.²⁶ The BIOSTAT-CHF risk model for predicting mortality included, age, blood urea nitrogen, NT-proBNP, haemoglobin and the use of a beta-blocker at time of inclusion. The BIOSTAT-CHF risk model for predicting mortality or HF hospitalization included age, NT-proBNP, haemoglobin, the use of a

beta-blocker at time of inclusion, a HF hospitalization in the year before inclusion, peripheral oedema, systolic blood pressure, high-density lipoprotein cholesterol, and sodium. Finally, to test whether cathepsin D improved this previous risk prediction model, we used Harrel's C index as well as the continuous net reclassification index and the integrative discrimination increment.

Experimental (*in vitro*) groups consisted of at least three biological replicates and technical duplicates were used. Data shown are expressed as the mean \pm standard error of the mean. As data were considered to be non-parametrical, differences between two groups were assessed by a Mann–Whitney U test, whereas comparisons between three or more groups were assessed with a Kruskal–Wallis test followed by Dunn's post-hoc test. A *P*-value of < 0.05 was considered statistically significant. Statistical analyses were performed using STATA 15.0 (College Station, TX, USA) and GraphPad Prism 7 (San Diego, CA, USA).

Results

Patient characteristics

Baseline characteristics of patients from the BIOSTAT-CHF index cohort according to tertiles of levels of cathepsin D are described in Table 1. Patients with higher levels of cathepsin D were in a more advanced New York Heart Association class, had worse signs and symptoms, and more often a history of atrial fibrillation or diabetes mellitus. Furthermore, patients with higher cathepsin D levels had lower levels of total cholesterol and higher levels of NT-proBNP, interleukin-6 and troponin T. In multivariable analyses, higher levels of cathepsin D were independently associated with a history of diabetes mellitus, higher levels of NT-proBNP, renin, and aspartate aminotransferase (Table 2). Clinical characteristics are shown in online supplementary Table S1 according to tertiles of cathepsin D in the validation cohort.

Outcome analyses

Median follow-up was after 21 months. In the BIOSTAT-CHF index cohort, 855 patients died or were hospitalized for HF (40%). The highest tertile of cathepsin D was associated with the highest rates of the primary combined outcome (Figure 1A) or all-cause mortality alone (Figure 1B). In multivariable analyses, higher levels of cathepsin D were independently associated with the primary combined outcome [hazard ratio (HR) 1.30; 95% confidence interval (CI) 1.19–1.43; $P < 0.001$] and all-cause mortality alone (HR 1.40; 95% CI 1.24–1.58; $P < 0.001$) (Table 2). When correcting for the BIOSTAT-CHF risk engine, higher levels of cathepsin D were independently associated with the combined outcome (HR 1.12; 95% CI 1.02–1.23; $P = 0.016$) and all-cause mortality alone (HR 1.15; 95% CI 1.01–1.29; $P = 0.028$) (Table 3). After further correcting for a history of diabetes, higher levels of cathepsin D remained significantly associated with the primary combined outcome (HR 1.15; 95% CI 1.02–1.30; $P = 0.022$). Similar to the index cohort, higher levels of cathepsin D showed an independent association with mortality (HR 1.47; 95% CI 1.27–1.69; $P < 0.001$) and the combined outcome in the validation cohort (HR 1.23; 95% CI 1.09–1.40; $P < 0.001$) when corrected for the BIOSTAT-CHF risk engine.

Human stem cell-derived cardiomyocytes released cathepsin D in response to stretch

To determine which stress-inducing conditions could induce cathepsin D release from hPSC-CM, we initially determined the effects of neurohormonal stimulation (as is similar in HF conditions) by incubating these hPSC-CM with incremental doses of angiotensin II, isoproterenol, and norepinephrine (online supplementary Figure S1). However, none of these stimuli induced cathepsin D release at physiological concentrations. In contrast, mechanical stretch and hypoxia resulted in increased levels of cathepsin D in the cell medium, while TNF α did not elicit any change in extracellular cathepsin D levels (Figure 2A). Strikingly, only hypoxia reduced intracellular levels of cathepsin D, while other conditions did not elicit any changes in intracellular cathepsin D (Figure 2B). To assess the relationship between extracellular cathepsin D levels and hPSC-CM death, the cardiac damage marker troponin T was quantified in the cell medium. Troponin T levels were found to be elevated after mechanical stretch, while troponin T levels were not significantly changed after TNF α stimulation or hypoxia compared to controls (Figure 2C).

Reduced cathepsin D expression resulted in impaired human stem cell-derived cardiomyocyte survival and sarcomeric structure

To assess the effects of reduced cathepsin D expression in response to stress, we applied shRNA-mediated targeted cathepsin D knockdown in hPSC-CM. We continued with the cyclic mechanical stretch model as it induced increased cathepsin D release *in vitro* and it has been extensively characterized as a representative model for wall stress leading to cardiac hypertrophy.²³ Viral RNA interference of cathepsin D resulted in an 88% reduction of intracellular cathepsin D protein levels compared to scrambled control hPSC-CM (shSCR; Figure 3A). Consequently, cathepsin D knockdown resulted in significantly reduced cathepsin D release from stretched hPSC-CM compared to stretched control hPSC-CM (Figure 3B). Cathepsin D knockdown resulted in increased troponin T levels in the medium of static hPSC-CM, which was exacerbated markedly after mechanical stretch (Figure 3C). We performed immunocytochemistry to morphologically assess hPSC-CM morphology based on sarcomeric structure, which also provided indications about how muscle fibres were affected in stretched hPSC-CM with and without cathepsin D silencing. To that end, we stained hPSC-CM for α -actinin and determined the ratio of sarcomeric structures based on three cardiomyocyte classes (Figure 3D and online supplementary Figure S2). We observed that knockdown of cathepsin D resulted in deterioration of sarcomeres independently of mechanical stretch. To determine the effects of cathepsin D knockdown on cell death, we measured the levels of apoptosis and necrosis (Figure 3E and 3F). Silencing of cathepsin D did not affect apoptosis, whereas necrosis was significantly increased after hPSC-CM with cathepsin D knockdown have been

Table 1 Baseline characteristics of patients from the BIOSTAT-CHF index cohort according to tertiles of cathepsin D

	1st tertile	2nd tertile	3rd tertile	P-value
<i>n</i>	725	725	724	
Demographics				
Age (years)	68.4 (12.2)	68.7 (11.8)	69.6 (12.2)	0.140
Female sex	213 (29.4%)	170 (23.4%)	198 (27.3%)	0.035
HF type				
HF _r EF	538 (80.3%)	531 (81.4%)	503 (80.6%)	0.910
HF _{mr} EF	85 (12.7%)	82 (12.6%)	76 (12.2%)	
HF _p EF	47 (7.0%)	39 (6.0%)	45 (7.2%)	
BMI (kg/m ²)	27.4 (5.4)	27.9 (5.4)	28.2 (5.7)	0.030
Ischaemic aetiology	306 (42.9%)	308 (43.6%)	337 (47.1%)	0.220
NYHA class				
I	75 (10.3%)	59 (8.1%)	51 (7.0%)	0.028
II	356 (49.1%)	337 (46.5%)	310 (42.8%)	
III	178 (24.6%)	209 (28.8%)	236 (32.6%)	
IV	23 (3.2%)	23 (3.2%)	29 (4.0%)	
NA	93 (12.8%)	97 (13.4%)	98 (13.5%)	
Systolic BP (mmHg)	125.1 (23.0)	124.1 (20.9)	124.3 (22.1)	0.640
Diastolic BP (mmHg)	74.9 (13.3)	75.2 (13.2)	74.0 (13.4)	0.190
LVEF (%)	31.5 (10.6)	30.7 (10.7)	31.1 (11.0)	0.450
Heart rate (bpm)	77.8 (18.3)	80.6 (20.8)	81.9 (19.5)	<0.001
Signs and symptoms				
Peripheral oedema				
Not present	287 (49.0%)	244 (41.6%)	202 (32.1%)	<0.001
Ankle	167 (28.5%)	189 (32.2%)	174 (27.7%)	
Below knee	105 (17.9%)	128 (21.8%)	174 (27.7%)	
Above knee	27 (4.6%)	26 (4.4%)	79 (12.6%)	
Elevated JVP	133 (25.7%)	140 (28.1%)	220 (41.3%)	<0.001
Hepatomegaly	89 (12.3%)	76 (10.5%)	137 (19.1%)	<0.001
Orthopnoea	197 (27.2%)	259 (35.8%)	298 (41.3%)	<0.001
Medical history				
Anaemia	244 (34.9%)	236 (34.3%)	279 (39.6%)	0.074
Atrial fibrillation	298 (41.1%)	348 (48.0%)	345 (47.7%)	0.012
Diabetes mellitus	198 (27.3%)	234 (32.3%)	269 (37.2%)	<0.001
COPD	107 (14.8%)	137 (18.9%)	129 (17.8%)	0.095
Hypertension	447 (61.7%)	452 (62.3%)	448 (61.9%)	0.960
PAVD	77 (10.6%)	79 (10.9%)	84 (11.6%)	0.830
Stroke	69 (9.5%)	57 (7.9%)	79 (10.9%)	0.140
PCI	143 (19.7%)	143 (19.7%)	163 (22.5%)	0.320
Medication				
Loop diuretics	719 (99.2%)	723 (99.7%)	721 (99.6%)	0.310
ACEi/ARB at baseline	528 (72.8%)	529 (73.0%)	502 (69.3%)	0.220
Beta-blocker at baseline	609 (84.0%)	603 (83.2%)	595 (82.2%)	0.650
Aldosterone antagonist	382 (52.7%)	399 (55.0%)	361 (49.9%)	0.140
Laboratory				
Haemoglobin (g/dL)	13.2 (1.8)	13.3 (1.9)	13.1 (2.0)	0.038
Total cholesterol (mmol/L)	4.3 (3.5, 5.1)	4.2 (3.4, 5.1)	3.8 (3.1, 4.9)	<0.001
IL-6 (pg/mL)	4 (2.4, 7.4)	5.1 (2.7, 9.5)	7.2 (4, 15.4)	<0.001
eGFR (mL/min/1.73 m ²)	64 (50, 80)	63 (47, 78)	57 (42, 76)	<0.001
Creatinine (μmol/L)	99 (81, 122)	104 (85, 129)	106 (87, 141)	<0.001
Sodium (mmol/L)	140.0 (138.0, 142.0)	140.0 (137.0, 142.0)	139.0 (136.0, 141.0)	<0.001
Potassium (mmol/L)	4.3 (3.9, 4.6)	4.3 (3.9, 4.6)	4.2 (3.9, 4.6)	0.014
HbA1c (%)	6.2 (5.6, 6.8)	6.2 (5.8, 7.2)	6.6 (5.9, 7.5)	0.006
NT-proBNP (ng/L)	3576.5 (2015.0, 7000.0)	3763.0 (2110.0, 7520.0)	5040.0 (2921.5, 9782.5)	<0.001
Troponin I (μg/L)	0.0 (0.0, 0.1)	0.0 (0.0, 0.1)	0.0 (0.0, 0.1)	0.012

ACEi, angiotensin-converting enzyme inhibitor; ARB, angiotensin receptor blocker; BMI, body mass index; BP, blood pressure; COPD, chronic obstructive pulmonary disease; eGFR, estimated glomerular filtration rate; HbA1c, glycated haemoglobin; HF, heart failure; HF_{mr}EF, heart failure with mid-range ejection fraction; HF_pEF, heart failure with preserved ejection fraction; HF_rEF, heart failure with reduced ejection fraction; IL-6, interleukin-6; JVP, jugular venous pressure; LVEF, left ventricular ejection fraction; NA, not available; NT-proBNP, N-terminal pro-B-type natriuretic peptide; NYHA, New York Heart Association; PAVD, peripheral arterial vascular disease; PCI, percutaneous coronary intervention.

Table 2 Clinical characteristics and laboratory values associated with cathepsin D

	Univariable		Multivariable	
	Beta	P-value	Beta	P-value
Age (years)	0.06	0.003	0.03	0.531
Sex	0.01	0.545		
BMI	0.06	0.004	0.10	0.013
Atrial fibrillation	0.08	<0.001	0.03	0.484
Hypertension	-0.02	0.316		
Diabetes	0.08	<0.001	0.08	0.049
eGFR	-0.09	<0.001	-0.08	0.059
NT-proBNP	0.15	<0.001	0.11	0.014
Aldosterone	0.01	0.786		
Renin	0.07	0.001	0.08	0.037
AST	0.20	<0.001	0.27	<0.001
ALT	0.09	0.001	-0.10	0.086
CRP	0.16	<0.001	0.05	0.236

ALT, alanine aminotransferase; AST, aspartate aminotransferase; BMI, body mass index; CRP, C-reactive protein; eGFR, estimated glomerular filtration rate; NT-proBNP, N-terminal pro-B-type natriuretic peptide;

mechanically stretched. Additionally, we observed that stretched hPSC-CM showed induction of autophagy, which was impaired in hPSC-CM with cathepsin D knockdown (Figure 3G). Furthermore, metabolism was found to be increased in stretched hPSC-CM with cathepsin D knockdown exclusively (Figure 3H).

Cathepsin D retention improved stretch-induced autophagy

To determine whether cathepsin D is actively secreted (i.e. exocytosis) or passively released (i.e. loss of membrane integrity) by stressed hPSC-CM, we incubated hPSC-CM with the lysosomal

inhibitor vacuolin-1 during mechanical stretch. As demonstrated previously, mechanical stretch induced cathepsin D release into the extracellular environment, whereas hPSC-CM incubated with vacuolin-1 did not show increased levels of released cathepsin D (Figure 4A). To assess the intracellular levels of cathepsin D protein, western blot was performed and we observed increased levels of intracellular cathepsin D after addition of vacuolin-1 (Figure 4B). As cathepsin D may be essential for the induction of stress responses, we investigated potential beneficial effects of vacuolin-1-mediated cathepsin D retention by measuring levels of apoptosis, necrosis, autophagy, and metabolism in stretched hPSC-CM with cathepsin D knockdown. We observed that apoptosis and necrosis (Figure 4C and 4D, respectively) were only marginally affected by the administration of vacuolin-1, but the ability to induce autophagy could be restored (Figure 4E). However, metabolic rates (i.e. cellular capacity to convert a pre-luminescent substrate to luminescent signal) remained unaffected by vacuolin-1 (Figure 4F).

Discussion

Our findings show that cathepsin D levels in patients with HF are associated with more advanced disease and higher rates of mortality and hospitalization for HF. Secondly, we found that cathepsin D is released by hPSC-CM following cardiac stretch in correspondence with troponin T release. Thirdly, silencing cathepsin D resulted in elevated levels of troponin T, especially following induced stress. These findings suggest that intracellular cathepsin D is essential for cardiomyocyte survival, while circulating cathepsin D levels are correlated to disease severity.

Elevated levels of most other cathepsins (i.e. CTSB, CTSF, CTSK, CTSL, CTSS, and CTSV) have been associated with cardiovascular diseases,²⁷⁻³³ but this is the first study showing that circulating levels of cathepsin D predict adverse outcomes in HF. In a human setting, higher levels of cathepsin D were associated with an increased risk of coronary events in the Malmö Diet and Cancer cardiovascular cohort.¹³ Similarly to our findings, cathepsin D levels were

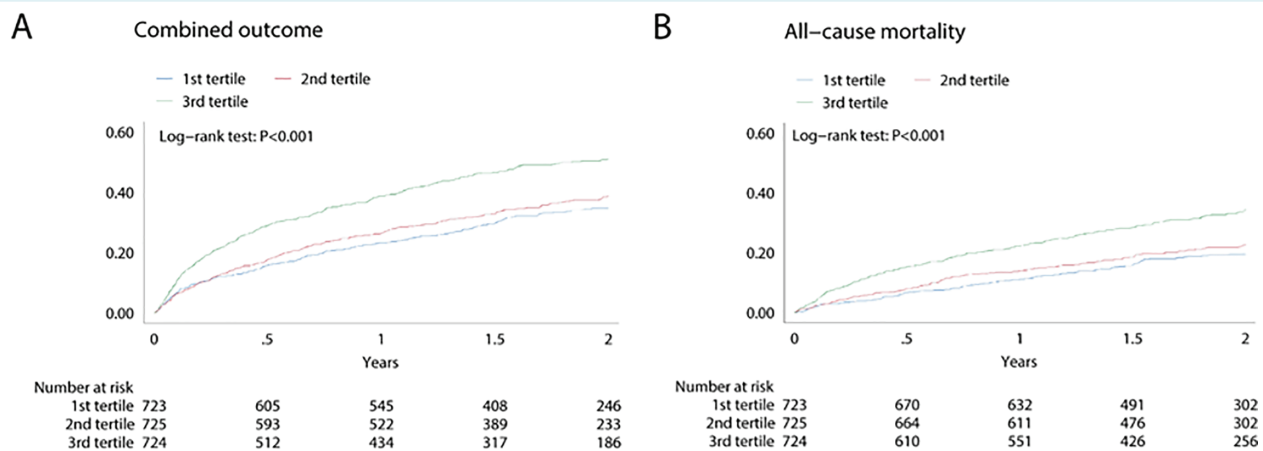


Figure 1 Cumulative incidence curves for the combined outcome of heart failure-related hospitalizations and/or all-cause mortality at 2 years (A) and all-cause mortality at 2 years (B).

Table 3 Hazard ratios in predicting the combined endpoint (heart failure hospitalizations or all-cause mortality at 2 years)

	Combined outcome		All-cause mortality	
	HR (95% CI)	P-value	HR (95% CI)	P-value
Univariable	1.38 (1.26–1.52)	<0.001	1.46 (1.30–1.64)	<0.001
Model 1	1.36 (1.24–1.49)	<0.001	1.41 (1.26–1.59)	<0.001
Model 2	1.31 (1.19–1.44)	<0.001	1.40 (1.25–1.58)	<0.001
Model 3	1.30 (1.19–1.43)	<0.001	1.40 (1.24–1.58)	<0.001
BIOSTAT-CHF risk model	1.12 (1.02–1.23)	0.016	1.15 (1.01–1.29)	0.028

CI, confidence interval; HR, hazard ratio.

Model 1 is adjusted for age and sex.

Model 2 is adjusted for model 1 + body mass index, country, history of hypertension, diabetes.

Model 3 is adjusted for model 2 + beta-blockers, angiotensin-converting enzyme inhibitor and mineralocorticoid receptor antagonist usage at baseline.

BIOSTAT-CHF risk model is adjusted for age, heart failure hospitalization in the year before inclusion, oedema, N-terminal pro-B-type natriuretic peptide, systolic blood pressure, haemoglobin, high-density lipoprotein levels, serum sodium concentration, and failure to prescribe a beta-blocker.

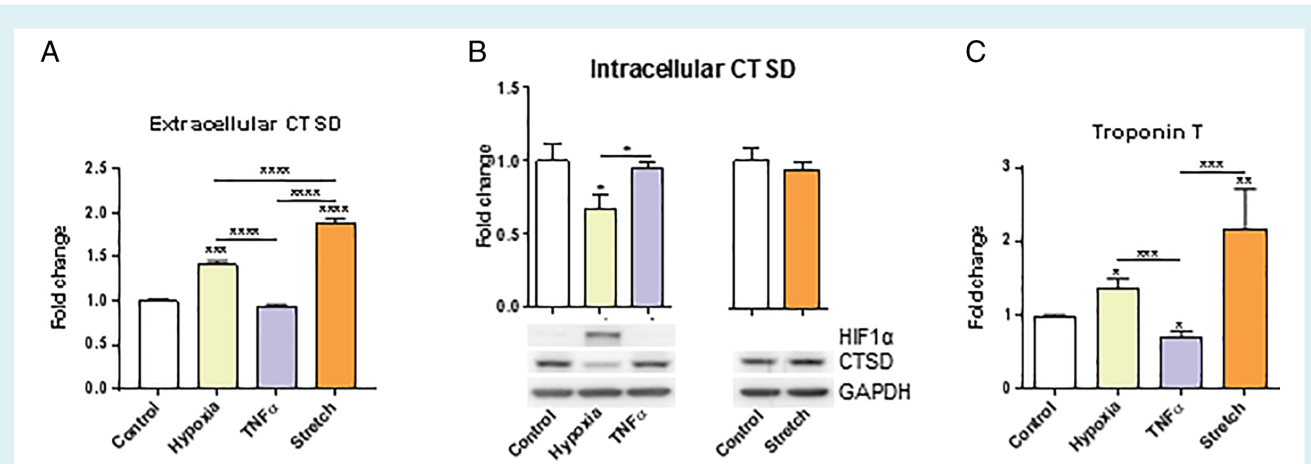


Figure 2 Cathepsin D (CTSD) was released by human stem cell-derived cardiomyocytes in concert with troponin T. Extracellular levels of CTSD were elevated after stretch (A), while intracellular levels were only reduced after tumour necrosis factor alpha (TNF α) stimulation or hypoxia (B). Damage marker release of troponin T was also increased by mechanical stretch (C). Graphs show results from three independent experiments; * $P < 0.05$; ** $P < 0.01$; *** $P < 0.001$ vs. unstimulated control human stem cell-derived cardiomyocytes unless otherwise indicated. Statistical analysis was done with with a Kruskal–Wallis test followed by Dunn's post-hoc test. HIF1 α , hypoxia-inducible factor 1 alpha.

associated with the presence of diabetes and other markers of the metabolic syndrome.¹³ Furthermore, cathepsin D was associated with atherosclerosis and carotid intima–media thickness.^{34,35} Most importantly, cathepsin D protein levels were found to be increased in explanted failing hearts from patients with ischaemic heart disease.¹¹ In a separate study, Naseem *et al.*³⁶ found that cathepsin D levels in patients with myocardial infarction were increased 7–20 h following myocardial infarction in concert with increased plasma renin activity. This study demonstrated that angiotensinogen can be converted to angiotensin I by circulating cathepsin D and thereby provides an alternative pathway to catalyse angiotensin II formation post-myocardial infarction. A previous study by Bouwens *et al.*³⁷ found an association of cathepsin D with adverse outcomes in 263 patients with chronic HF. We extend upon these previous findings in several ways: (i) our study provides results on the clinical correlates and prognostic value of cathepsin D in a large, well

characterized, multinational, prospective study with independent validation; (ii) results of the present study show evidence supporting that active cardiac excretion of cathepsin D is associated with adverse clinical outcomes.

A previous study by Wu *et al.*¹¹ investigated the role of cathepsin D in ischaemic heart disease and observed a detrimental effect of cathepsin D knockout. In their study, cathepsin D^{+/-} mice displayed reduced autophagic flux following myocardial infarction and a diastolic dysfunction. Based on this study and on the ubiquitous expression of cathepsin D, we hypothesized that cathepsin D is essential for cellular stress responses and coping mechanisms for cardiomyocytes in order to survive and maintain adequate contractile function. To determine the specific effects of cathepsin D ablation in hPSC-CM, we transduced hPSC-CM with a cathepsin D-specific shRNA resulting in cathepsin D knockdown. We expected that

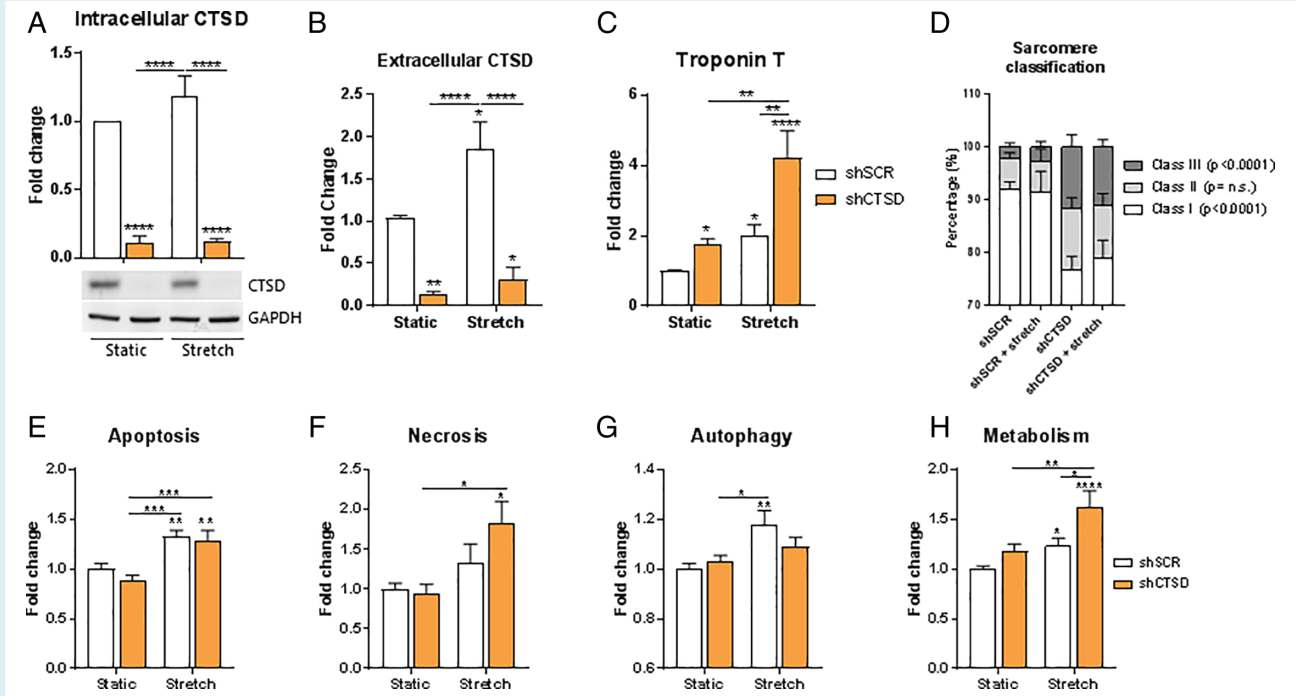


Figure 3 Cathepsin D (CTSD) knockdown resulted in increased cell death following mechanical stretch. Intracellular levels of CTSD were greatly reduced by shRNA-mediated CTSD gene silencing (A); extracellular levels were found to show a similar pattern (B). Troponin T levels were found to be increased following mechanical stretch with CTSD knockdown (C). CTSD knockdown resulted in deteriorated sarcomeric structure (D). Mechanical stretch induced apoptosis regardless of CTSD knockdown (E), whereas necrosis is increased after stretch in human stem cell-derived cardiomyocytes (hPSC-CM) with CTSD knockdown (F). Stretching induced autophagy in scrambled control hPSC-CM, which was abrogated in CTSD-deficient cells (G). Stretching resulted in increased metabolism in hPSC-CM with CTSD silencing exclusively (GH). Graphs show results from three independent experiments; * $P < 0.05$; ** $P < 0.01$; *** $P < 0.001$; **** $P < 0.0001$ vs. static scrambled control hPSC-CM (shSCR) unless otherwise indicated. Statistical analysis was done with with a Kruskal–Wallis test followed by Dunn’s post-hoc test.

severely reduced cathepsin D levels would induce cellular damage due to aberrant proteolysis or protein accumulation (as seen in neurodegenerative disorders).³⁸ We observed increased levels of troponin T in the cell medium of hPSC-CM with cathepsin D knockdown (without mechanical stretch), indicating that cardiomyocyte survival is reduced due to cathepsin D deficiency. Interestingly, cathepsin D knockdown resulted in a striking increase of extracellular troponin T levels following mechanical stretch, as well as increased necrosis and impaired induction of autophagy. Inhibition of lysosomal exocytosis prevented active cathepsin D secretion and retention of intracellular cathepsin D. While this restored the ability of stressed hPSC-CM to induce autophagy, we argue that general (and non-specific) inhibition of lysosomal exocytosis may hamper stress-induced lysosomal-dependent coping mechanisms that may be more important to cell survival compared to increased levels of cathepsin D as a factor in autophagy. Additionally, reduction of cathepsin D resulted in deteriorated sarcomeric structures that may contribute to HF progression. Our data indicate that cathepsin D is necessary for cardiomyocyte survival, especially during stress. These findings are in line with the previously mentioned study by Wu *et al.*¹¹ Moreover, apoptosis and necrosis were significantly increased following cathepsin D silencing, while stress-induced autophagy was abrogated. Combined, these results

suggest that regulated cell death (i.e. apoptosis) is dependent on autophagy as part of the stress response. Abrogated cathepsin D function might, therefore, lead to uncontrolled cell death and increased stress-induced metabolism.

The present study applied various methods to induce cellular stress responses. Since mechanical stretch resulted in the highest levels of cathepsin D in cell medium, we opted to continue with this well characterized and representative cardiac stress model to study the effects of cathepsin D knockdown (i.e. mechanical stretch). Both the present study and the study by Wu *et al.* caused cathepsin D deficiencies in cardiomyocytes and mice, respectively, which has not yet been proven to be representative for HF patients. It is clear that insufficient intracellular levels of cathepsin D are detrimental for stress responses and subsequent cardiomyocyte survival. We observed no differences in intracellular cathepsin D levels after mechanical stretch, while extracellular levels were significantly increased.

Limitations

Due to the relative nature of the methodology used to determine biomarker levels, no absolute cathepsin D levels are known. As a result, it is not possible to determine absolute thresholds that

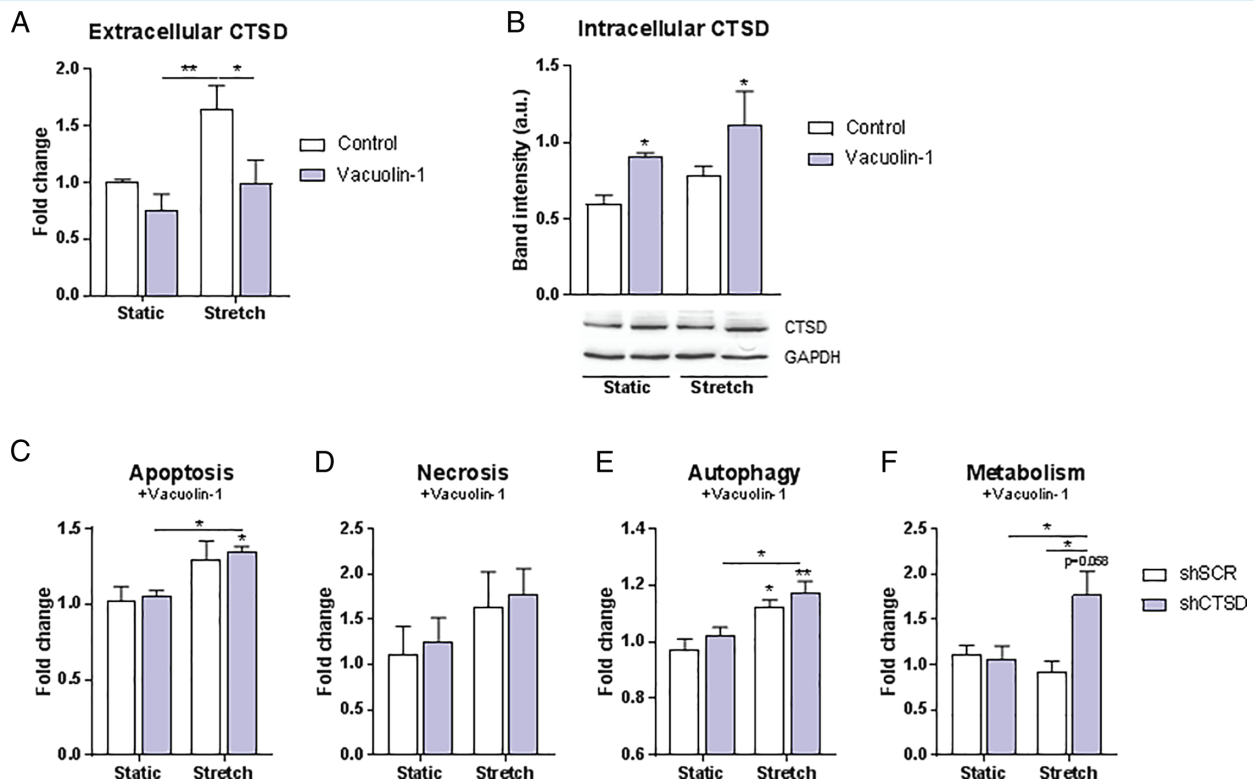


Figure 4 Inhibition of lysosomal exocytosis by vacuolin-1 improved autophagic response by retention of intracellular cathepsin D (CTSD). Extracellular levels of CTSD after stretch were reduced compared to stretched vehicle control stem cell-derived cardiomyocytes (hPSC-CM) (A). Incubation with vacuolin-1 increased intracellular levels of CTSD (B). Inhibition of CTSD secretion marginally affected apoptosis (C) and prevented induction of necrosis (D). Autophagy was restored by vacuolin-1 in CTSD knockdown hPSC-CM after stretch (E), whereas metabolism was unaffected (F). Graphs show results from three independent experiments; * $P < 0.05$; ** $P < 0.01$ vs. static scrambled control hPSC-CM (shSCR) unless otherwise indicated. Statistical analysis was done with a Kruskal–Wallis test followed by Dunn's post-hoc test.

can be used for prognostic purposes. Moreover, we cannot draw any conclusions regarding the effects of abolished cathepsin D in other cell types based on the experiments performed in this study. Notably, Wu *et al.*¹¹ studied the effects of cathepsin D in ablation in global heterozygous knockout mice after coronary artery ligation. Therefore, the observed effects in that study could also arise from detrimental effects on other cell types, e.g. endothelial function is closely associated with cardiomyocyte function. The observed adverse effects on cardiac function in the study of Wu *et al.* could have arisen from endothelial damage as opposed to direct myocardial effects. It remains unknown whether patients with high levels of circulating cathepsin D concurrently have reduced intracellular levels of cathepsin D. However, it is not feasible to determine intracellular cathepsin D levels in the heart at the time of blood collection.

Finally, the validation cohort was slightly older with a higher ejection fraction and lower B-type natriuretic peptide levels. This is a limitation, because it might inflate the type II error, but also a particular strength because the association of cathepsin D with adverse clinical outcomes was shown in two independent cohorts with slight differences in age, ejection fraction and disease severity.

Conclusions

In patients with HF, higher circulating cathepsin D levels correlate with greater disease severity. Our *in vitro* studies suggest that cathepsin D is secreted from hPSC-CM following hypoxia and mechanical stretch and that cathepsin D is necessary for (autophagy-mediated) human stem cell-derived cardiomyocyte survival, especially during stress.

Supplementary Information

Additional supporting information may be found online in the Supporting Information section at the end of the article.

Acknowledgements

We gratefully acknowledge Martin Dokter for excellent technical assistance.

Funding

BIOSTAT-CHF was funded by a grant from the European Commission (FP7-242209-BIOSTAT-CHF; EudraCT 2010–020808–29).

Conflict of interest: none declared.

References

- van der Pol A, van Gilst WH, Voors AA, van der Meer P. Treating oxidative stress in heart failure: past, present and future. *Eur J Heart Fail* 2019;**21**:425–435.
- Qin F, Lennon-Edwards S, Lancel S, Biolo A, Siwik DA, Pimentel DR, Dorn GW, Kang YJ, Colucci WS. Cardiac-specific overexpression of catalase identifies hydrogen peroxide-dependent and -independent phases of myocardial remodeling and prevents the progression to overt heart failure in G(alpha)q-overexpressing transgenic mice. *Circ Heart Fail* 2010;**3**:306–313.
- Patel RS, Ghasemzadeh N, Eapen DJ, Sher S, Arshad S, Ko Y, Veledar E, Samady H, Zafari AM, Sperling L, Vaccarino V, Jones DP, Quyyumi AA. Novel biomarker of oxidative stress is associated with risk of death in patients with coronary artery disease. *Circulation* 2016;**133**:361–369.
- Lu Z, Xu X, Hu X, Lee S, Traverse JH, Zhu G, Fassett J, Tao Y, Zhang P, dos Remedios C, Pritzker M, Hall JL, Garry DJ, Chen Y. Oxidative stress regulates left ventricular PDE5 expression in the failing heart. *Circulation* 2010;**121**:1474–1483.
- Forgione MA, Cap A, Liao R, Moldovan NI, Eberhardt RT, Lim CC, Jones J, Goldschmidt-Clermont PJ, Loscalzo J. Heterozygous cellular glutathione peroxidase deficiency in the mouse: abnormalities in vascular and cardiac function and structure. *Circulation* 2002;**106**:1154–1158.
- Diment S, Martin KJ, Stahl PD. Cleavage of parathyroid hormone in macrophage endosomes illustrates a novel pathway for intracellular processing of proteins. *J Biol Chem* 1989;**264**:13403–13406.
- Barrett AJ. Cathepsin D. Purification of isoenzymes from human and chicken liver. *Biochem J* 1970;**117**:601–607.
- Li DL, Wang ZV, Ding G, Tan W, Luo X, Criollo A, Xie M, Jiang N, May H, Kyrychenko V, Schneider JW, Gillette TG, Hill JA. Doxorubicin blocks cardiomyocyte autophagic flux by inhibiting lysosome acidification. *Circulation* 2016;**133**:1668–1687.
- Laurent-Matha V, Derocq D, Prébois C, Katunuma N, Liaudet-Coopman E. Processing of human cathepsin D is independent of its catalytic function and auto-activation: involvement of cathepsins L and B. *J Biochem* 2006;**139**:363–371.
- Metcalf P, Fusek M. Two crystal structures for cathepsin D: the lysosomal targeting signal and active site. *EMBO J* 1993;**12**:1293–1302.
- Wu P, Yuan X, Li F, Zhang J, Zhu W, Wei M, Li J, Wang X. Myocardial upregulation of cathepsin D by ischemic heart disease promotes autophagic flux and protects against cardiac remodeling and heart failure. *Circ Heart Fail* 2017;**10**:e004044.
- Ma X, Liu H, Foyil SR, Godar RJ, Weinheimer CJ, Hill JA, Diwan A. Impaired autophagosome clearance contributes to cardiomyocyte death in ischemia/reperfusion injury. *Circulation* 2012;**125**:3170–3181.
- Gonçalves I, Hultman K, Dunér P, Edseldt A, Hedblad B, Fredrikson GN, Björkbacka H, Nilsson J, Bengtsson E. High levels of cathepsin D and cystatin B are associated with increased risk of coronary events. *Open Heart* 2016;**3**:e000353.
- Yamac AH, Sevgili E, Kucukbuzcu S, Nasifov M, Ismailoglu Z, Kilic E, Ercan C, Jafarov P, Uyarel H, Bacaksiz A. Role of cathepsin D activation in major adverse cardiovascular events and new-onset heart failure after STEMI. *Herz* 2015;**40**:912–920.
- Voors AA, Anker SD, Cleland JG, Dickstein K, Filippatos G, van der Harst P, Hillege HL, Lang CC, Ter Maaten JM, Ng L, Ponikowski P, Samani NJ, van Veldhuisen DJ, Zannad F, Zwiderman AH, Metra M. A systems BIOlogy study to Tailored treatment in chronic heart failure: rationale, design, and baseline characteristics of BIOSTAT-CHF. *Eur J Heart Fail* 2016;**18**:716–726.
- Ouwerkerk W, Voors AA, Anker SD, Cleland JG, Dickstein K, Filippatos G, van der Harst P, Hillege HL, Lang CC, Ter Maaten JM, Ng LL, Ponikowski P, Samani NJ, van Veldhuisen DJ, Zannad F, Metra M, Zwiderman AH. Determinants and clinical outcome of uptitration of ACE-inhibitors and beta-blockers in patients with heart failure: a prospective European study. *Eur Heart J* 2017;**38**:1883–1890.
- Tromp J, Westenbrink BD, Ouwerkerk W, van Veldhuisen DJ, Samani NJ, Ponikowski P, Metra M, Anker SD, Cleland JG, Dickstein K, Filippatos G, van der Harst P, Lang CC, Ng LL, Zannad F, Zwiderman AH, Hillege HL, van der Meer P, Voors AA. Identifying pathophysiological mechanisms in heart failure with reduced versus preserved ejection fraction. *J Am Coll Cardiol* 2018;**72**:1081–1090.
- Tromp J, Ouwerkerk W, Demissei BG, Anker SD, Cleland JG, Dickstein K, Filippatos G, van der Harst P, Hillege HL, Lang CC, Metra M, Ng LL, Ponikowski P, Samani NJ, van Veldhuisen DJ, Zannad F, Zwiderman AH, Voors AA, van der Meer P. Novel endotypes in heart failure: effects on guideline-directed medical therapy. *Eur Heart J* 2018;**39**:4269–4276.
- Assarsson E, Lundberg M, Holmquist G, Björkesten J, Thorsen SB, Ekman D, Eriksson A, Rennel Dickens E, Ohlsson S, Edfeldt G, Andersson A-C, Lindstedt P, Stenvang J, Gullberg M, Fredriksson S. Homogenous 96-plex PEA immunoassay exhibiting high sensitivity, specificity, and excellent scalability. *PLoS One* 2014;**9**:e95192.
- Beusekamp JC, Tromp J, van der Wal HH, Anker SD, Cleland JG, Dickstein K, Filippatos G, van der Harst P, Hillege HL, Lang CC, Metra M, Ng LL, Ponikowski P, Samani NJ, van Veldhuisen DJ, Zwiderman AH, Rossignol P, Zannad F, Voors AA, van der Meer P. Potassium and the use of renin-angiotensin-aldosterone system inhibitors in heart failure with reduced ejection fraction: data from BIOSTAT-CHF. *Eur J Heart Fail* 2018;**20**:923–930.
- Hoes MF, Grote Beverborg N, Kijlstra JD, Kuipers J, Swinkels DW, Giepmans BN, Rodenburg RJ, van Veldhuisen DJ, de Boer RA, van der Meer P. Iron deficiency impairs contractility of human cardiomyocytes through decreased mitochondrial function. *Eur J Heart Fail* 2018;**20**:910–919.
- Burridge PW, Matsa E, Shukla P, Lin ZC, Churko JM, Ebert AD, Lan F, Diecke S, Huber B, Mordwinkin NM, Plews JR, Abilez OJ, Cui B, Gold JD, Wu JC. Chemically defined generation of human cardiomyocytes. *Nat Methods* 2014;**11**:855–860.
- Ovchinnikova E, Hoes M, Ustyantsev K, Bomer N, de Jong TV, van der Mei H, Berezikov E, van der Meer P. Modeling human cardiac hypertrophy in stem cell-derived cardiomyocytes. *Stem Cell Reports* 2018;**10**:794–807.
- Cerny J, Feng Y, Yu A, Miyake K, Borgonovo B, Klumperman J, Meldolesi J, McNeil PL, Kirchhausen T. The small chemical vacuolin-1 inhibits Ca²⁺-dependent lysosomal exocytosis but not cell resealing. *EMBO Rep* 2004;**5**:883–888.
- Birkett MJ, Casini S, Kosmidis G, Elliott DA, Gerencsér AA, Baartscheer A, Schumacher C, Mastroberardino PG, Elefant AG, Stanley EG, Mummery CL. PGC-1 α and reactive oxygen species regulate human embryonic stem cell-derived cardiomyocyte function. *Stem Cell Reports* 2013;**1**:560–574.
- Voors AA, Ouwerkerk W, Zannad F, van Veldhuisen DJ, Samani NJ, Ponikowski P, Ng LL, Metra M, ter Maaten JM, Lang CC, Hillege HL, van der Harst P, Filippatos G, Dickstein K, Cleland JG, Anker SD, Zwiderman AH. Development and validation of multivariable models to predict mortality and hospitalization in patients with heart failure. *Eur J Heart Fail* 2017;**19**:627–634.
- Abd-Elrahman I, Meir K, Kosuge H, Ben-Nun Y, Weiss Sadan T, Rubinstein C, Samet Y, McConnell MV, Blum G. Characterizing cathepsin activity and macrophage subtypes in excised human carotid plaques. *Stroke* 2016;**47**:1101–1108.
- Yasuda Y, Li Z, Greenbaum D, Bogoy M, Weber E, Brömme D. Cathepsin V, a novel and potent elastolytic activity expressed in activated macrophages. *J Biol Chem* 2004;**279**:36761–36770.
- Liu J, Sukhova GK, Yang JT, Sun J, Ma L, Ren A, Xu WH, Fu H, Dolganov GM, Hu C, Libby P, Shi GP. Cathepsin L expression and regulation in human abdominal aortic aneurysm, atherosclerosis, and vascular cells. *Atherosclerosis* 2006;**184**:302–311.
- Oörni K, Sneek M, Brömme D, Pentikäinen MO, Lindstedt KA, Mäyränpää M, Aitio H, Kovanen PT. Cysteine protease cathepsin F is expressed in human atherosclerotic lesions, is secreted by cultured macrophages, and modifies low density lipoprotein particles in vitro. *J Biol Chem* 2004;**279**:34776–34784.
- Liu J, Sukhova GK, Sun JS, Xu WH, Libby P, Shi GP. Lysosomal cysteine proteases in atherosclerosis. *Arterioscler Thromb Vasc Biol* 2004;**24**:1359–1366.
- Platt MO, Ankeny RF, Shi GP, Weiss D, Vega JD, Taylor WR, Jo H. Expression of cathepsin K is regulated by shear stress in cultured endothelial cells and is increased in endothelium in human atherosclerosis. *Am J Physiol Heart Circ Physiol* 2007;**292**:H1479–H1486.
- Keegan PM, Surapaneni S, Platt MO. Sickle cell disease activates peripheral blood mononuclear cells to induce cathepsins K and V activity in endothelial cells. *Anemia* 2012;**2012**:201781.
- Moallem SA, Nazemian F, Elasi S, Alamdaran SA, Shamsara J, Mohammadpour AH. Correlation between cathepsin D serum concentration and carotid intima-media thickness in hemodialysis patients. *Int Urol Nephrol* 2011;**43**:841–848.
- Luis AJ. Atherosclerosis. *Nature* 2000;**407**:233–241.
- Naseem RH, Hedegard W, Henry TD, Lessard J, Sutter K, Katz SA. Plasma cathepsin D isoforms and their active metabolites increase after myocardial infarction and contribute to plasma renin activity. *Basic Res Cardiol* 2005;**100**:139–146.
- Bouwens E, Brankovic M, Mouthaan H, Baart S, Rizopoulos D, van Boven N, Caliskan K, Manintveld O, Germans T, van Ramshorst J, Umans V, Akkerhuis KM, Kardys I. Temporal patterns of 14 blood biomarker candidates of cardiac remodeling in relation to prognosis of patients with chronic heart failure – the Bio-SHiFT study. *J Am Heart Assoc* 2019;**8**:e009555.
- Vidoni C, Follo C, Savino M, Melone MAB, Isidoro C. The role of cathepsin D in the pathogenesis of human neurodegenerative disorders. *Med Res Rev* 2016;**36**:845–870.